Nuclear Mathematical and Computational Sciences: A Century in Review, A Century Anew
Gatlinburg, Tennessee, April 6-11, 2003, on CD-ROM, American Nuclear Society, LaGrange Park, IL (2003)

DEVELOPMENT AND APPLICATIONS OF THE SP_L METHODOLOGY FOR A CRITICALITY EIGENVALUE BENCHMARK PROBLEM

Gianluca Longoni, Glenn Sjoden, and Alireza Haghighat
University of Florida
Nuclear & Radiological Engineering Department
202 Nuclear Sciences Building
Gainesville, FL 32611
USA
longoni@ufl.edu, joedean@sprintmail.com, haghighat@ufl.edu

ABSTRACT

The SP_L equations have received renewed interest in reactor physics applications due to their inherent capability of including better transport physics when compared to diffusion equation. Moreover, the solution of the SP_L equations requires less overall computational effort compared to the S_N or P_N methodologies. In previous work by the authors, we derived the 3-D SP_3 equations, starting from the P_3 equations in 1-D geometry. In this paper, we derive the 3-D SP_L equations from the even-parity form of the S_N equations; these were implemented in the $PENSP_L$ code. Further, we compare the solutions of the SP_L, S_N, and Monte Carlo methodologies for a criticality eigenvalue benchmark problem (NEACRP-L-330), and discuss the advantages and limitations of the SP_L equations. We demonstrate that SP_3 is the minimum order that should be considered for a given problem; also, while accurate for most problems, use of the SP_L method to solve problems with void regions must be carefully evaluated, regardless of the SP_L order applied.

Key Words: Discrete Ordinates, Simplified P_N, SP_L, Criticality Calculation.

1. INTRODUCTION

The SP_L equations were initially proposed by Gelbard [1] in the early 1960s. Following their introduction, they did not receive much attention due to weak theoretical support. Recently, the SP_L equations have received more attention because they have been shown to provide more accurate solutions compared to the diffusion equation. Moreover, the theoretical foundations of the SP_L equations have been significantly strengthened in recent years using a variational analysis approach in the derivation [4,5].

In a previous paper [2], we derived the 3-D SP_3 equations, starting from the 1-D P_3 equations and by applying the Gelbard procedure; we implemented these equations in the $PENSP_3$ (Parallel Environment Neutral-particle SP_3 code [2]). The structure of these equations is characterized by a second order elliptic operator, which makes them amenable to a solution with standard iterative techniques, such as preconditioned conjugate gradient methods. In this paper, we will derive the SP_L equations, starting from the even-parity form of the 1-D S_N (N=L+1) transport equations. Morel, Larsen and McGhee obtained the SP_L equations in a similar fashion [6]. The derivation of the SP_L equations starting from the even-parity form of the S_N equations presents many

advantages that are shared by the alternative derivation we presented in Ref. [2]. However, we note a distinctive property in the new derivation; the fluxes are mathematically decoupled on the boundary. This property allowed us to easily modify the $PENSP_3$ code to accommodate an arbitrary SP_L order.

We utilized the new code, $PENSP_L$ (Parallel Environment Neutral-particle SP_L code) to solve a criticality eigenvalue benchmark problem proposed by T. Takeda and H. Ikeda [7]. The problem selected is model no. 1 in the 3-D Neutron Transport Benchmarks designated as NEACRP-L-330. The problem consists of a simple core geometry representing a small LWR, with the presence of a control rod. We considered two different situations, in the first case with the control rod withdrawn (the "Control Rod-Out" case), while in the second case the rod is fully inserted (the "Control Rod-In" case). We used this problem to compare the accuracy of the SP_L equations versus the discrete ordinates (S_N) methodology. We solved the S_N equations using the PENTRAN Code System [3].

The remainder of this paper is organized as follows: Section 2 discusses the derivation of the SP_L equations starting from the even-parity form of the S_N equations and their implementation in the $PENSP_L$ code; Section 3 presents the benchmark problem, and Section 4 analyzes the results. Section 5 concludes the paper, and provides a few final remarks.

2. DERIVATION OF THE SP_L EQUATIONS FROM THE EVEN-PARITY S_N EQUATIONS

Currently, we have expanded on our work with the SP_3 equations and have derived the Simplified P_L (SP_L) equations commencing from the even-parity formulation of the transport equation. Subsequently, to experiment with the generalized SP_L formulation, we upgraded the $PENSP_3$ code to a generalized $PENSP_L$ (Parallel Environment Neutral-particle SP_L) code. The S_N transport equations in 1-D geometry are given by Eqs. 1.

$$
\begin{aligned}
&\mu_m \frac{\partial \psi(x,\mu_m)}{\partial x} + \sigma_t(x)\psi(x,\mu_m) = Q_m(x) \\
&Q_m(x) = \sum_{n=0}^{L} \frac{2n+1}{2} \sigma_{sn}(x)\phi_n(x)P_n(\mu_m) + q_m(x) + q_f(x) \\
&q_m = \sum_{n=0}^{L} \frac{2n+1}{2} S_n(x)P_n(\mu_m) \\
&q_f(x) = \frac{1}{k}\nu\sigma_f(x)\phi_0(x) \\
&\phi_n(x) = \sum_{n=1}^{L} w_m P_n(\mu_m)\psi(x,\mu_m) \\
&m = 1,2,...,N
\end{aligned}
\tag{1}
$$

In Eq.1, m is the angular index; $\{\mu_m, w_m\}$ are the corresponding roots and weights of the N-point quadrature formula. Eqs. 1 can be rewritten using the even-parity formulation as follows:

$$\mu_m \frac{\partial \psi(x,\mu_m)}{\partial x} + \sigma_t(x)\psi(x,\mu_m) = Q_m(x) \tag{2}$$

$$-\mu_m \frac{\partial \psi(x,-\mu_m)}{\partial x} + \sigma_t(x)\psi(x,-\mu_m) = Q_m(x) \tag{3}$$

The even-parity and odd-parity angular fluxes are shown in Eqs. 4a and 4b respectively.

$$\psi_m^+ = \frac{1}{2}\left[\psi(x,\mu_m) + \psi(x,-\mu_m)\right] \tag{4a}$$

$$\psi_m^- = \frac{1}{2}\left[\psi(x,\mu_m) - \psi(x,-\mu_m)\right] \tag{4b}$$

$$Q_m^+ = \frac{1}{2}\left[Q(x,\mu_m) + Q(x,-\mu_m)\right] \tag{4c}$$

$$Q_m^- = \frac{1}{2}\left[Q(x,\mu_m) - Q(x,-\mu_m)\right] \tag{4d}$$

Using Eqs. 2 and 3 and definitions 4a – 4d, we derive the even-parity form of the S_N transport equations given by Eqs. 5.

$$\mu_m \frac{\partial \psi_m^-}{\partial x} + \sigma_t \psi_m^+ = Q_m^+ \tag{5a}$$

$$\mu_m \frac{\partial \psi_m^+}{\partial x} + \sigma_t \psi_m^- = Q_m^- \tag{5b}$$

Using Eq. 5b, we obtain the odd-parity angular flux:

$$\psi_m^- = \frac{Q_m^-}{\sigma_t} - \frac{\mu_m}{\sigma_t}\frac{\partial \psi_m^+}{\partial x} \tag{6}$$

Then, we derive an even-parity equation by substituting Eq. 6 into Eq. 5a

$$-\frac{\partial}{\partial x}\frac{\mu_m^2}{\sigma_t}\frac{\partial \psi_m^+}{\partial x} + \sigma_t \psi_m^+ = Q_m^+ - \mu_m \frac{\partial}{\partial x}\left(\frac{Q_m^-}{\sigma_t}\right) \qquad m = 1,2..,\frac{N}{2} \tag{7}$$

The SP_L equations, in 3-D geometry, are obtained by substituting the gradient operator in place of the derivative operator in Eq. 7, as given by Eq. 8.

$$-\vec{\nabla}\frac{\mu_m^2}{\sigma_t(\vec{r})}\vec{\nabla}\psi_m^+(\vec{r})+\sigma_t(\vec{r})\psi_m^+(\vec{r})=Q_m^+(\vec{r})-\mu_m\vec{\nabla}\cdot\frac{Q_m^-(\vec{r})}{\sigma_t(\vec{r})}$$
$$m=1,2..,\frac{N}{2} \tag{8}$$

The vacuum boundary conditions are obtained simply by setting the incoming angular flux on the boundary surface equal to zero:

$$\psi_b(-\mu_m)=\psi_b^+(\mu_m)-\hat{n}\cdot\vec{F}_b(\mu_m)=0$$
$$or \tag{9}$$
$$\psi_b^+(\mu_m)=\hat{n}\cdot\vec{F}_b(\mu_m)$$

In Eq. 9, we have defined the SP_L odd-parity angular fluxes $\vec{F}_b$; they differ from the odd-parity S_N angular fluxes, because the angular behavior is represented by a truncated Legendre expansion instead of spherical harmonics. The reflective (symmetry) boundary condition is given by Eq. 10.

$$\hat{n}\cdot\vec{F}_b(\mu_m)=0 \tag{10}$$

We discretized the SP_L equations with the finite volume technique and implemented them in the new $PENSP_L$ code. We implemented the SPL equations in a 3-D Cartesian geometry using a Block-Adaptive Mesh Refinement (Block-AMR); the Block-AMR approach allows the user to specify a variable fine mesh structure for each coarse mesh in the model.
The linear system of equations arising from the spatial discretization is solved using the Conjugate Gradient method preconditioned with the Incomplete Cholesky factorization of the sparse matrix. The Cholesky factorization effectively reduced the number of iterations needed to reach convergence for the CG algorithm. Moreover, we optimized the memory allocation of the arrays with a Compressed Diagonal Storage technique; this methodology reduced also the number of operations required in the matrix-vector multiplication algorithm.
We parallelized the code for Distributed Memory Architectures using a moment decomposition strategy. In our implementation, we distribute the moments on the processors available. After a sweep is performed on each coarse mesh, the processors exchange the moments that were locally processed until convergence is reached.

3. NUMERICAL BENCHMARK

We have selected the problem 1 from collection [7] of 3-D benchmark problems, NEACRP-L-330 proposed by T. Takeda and H. Ikeda. The purpose of these problems is to validate the accuracy of present transport codes for criticality calculations. Problem 1 consists of a 3-D model of the Kyoto University Critical Assembly (KUCA). The core is composed by 93 w/o enriched U-Al alloy and natural uranium metal plates; the average U-235 enrichment is 9.6 w/o and the moderator is polyethylene. The core is symmetric about the origin and the dimensions are, in one octant, 15cm x 15cm x 15cm. A control rod (CR) is introduced outside of the core in

the reflector region. The model cross sections over x-y plane and x-z plane are shown in Figs. 1 and 2 respectively (dimensions are in centimeters).

The characteristics of this problem make it challenging for the SP_L equations; the presence of the void region involves long streaming paths, while the control rod produces steep thermal flux gradients at the interface. We compare the results obtained using the SP_L and S_N methods with those presented in Ref. 7 using the Monte Carlo method.

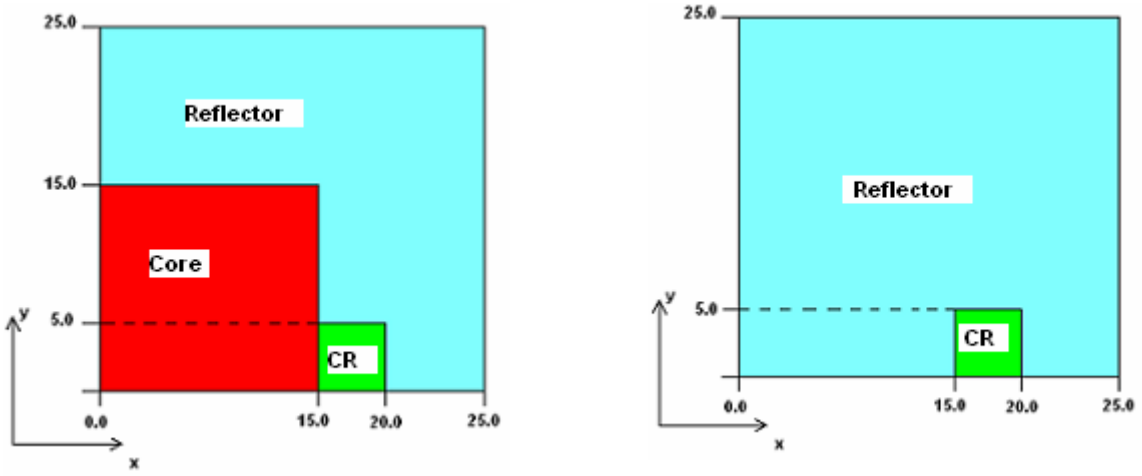

Figure 1. Model cross section on the x-y plane (left - z=0.0…15.0cm; right - z=15.0…25.0cm)

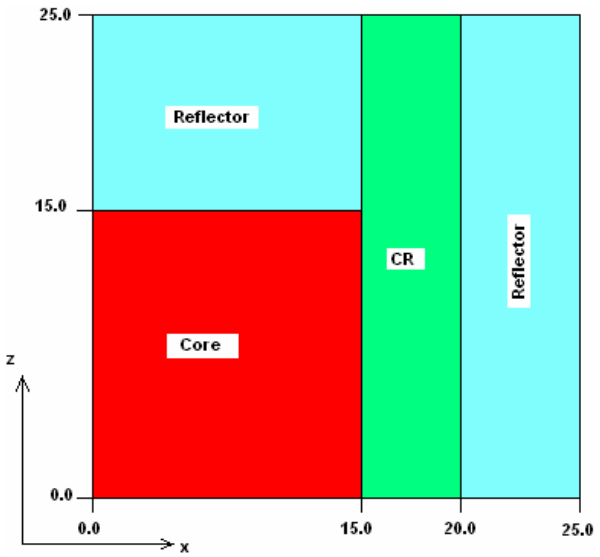

Figure 2. Model cross section on the x-z plane.

We have considered two cases with different configurations of the control rod; in the first case, the control rod is fully withdrawn and region is left empty (voided); in the second case, the

control rod is fully inserted into the system. Hence, we evaluated the control rod worth, defined by Eq. 11.

$$CRW = \left(\frac{1}{k_{eff}}\right)_{Case2} - \left(\frac{1}{k_{eff}}\right)_{Case1} \tag{11}$$

We have used the two-group cross sections provided in the benchmark problem [7]; note that the P_1 scattering effect has been included by using the transport cross section in place of the total cross section. Table I gives the convergence criteria for the inner and outer iterations for the S_N and SP_L calculations.

Table I. Criticality eigenvalues

Methodology	Inner Tolerance	Outer Tolerance
S_N	1.0E-4	1.0E-5
SP_L	1.0E-3	1.0E-5

We divided the model into two coarse z-levels; the first z-level spans from z=0.0 cm to z=15.0 cm, while the second z-level ranges from z=15.0 cm to z=25.0 cm. We used the linear Diamond differencing with zero fixup (DZ) in PENTRAN, and a linear averaged formulation in PENSP$_L$. The model is consistently discretized with a 1-cm uniform mesh along the three axes for each method.

4. RESULTS

In Table II, we show the criticality eigenvalues and the errors relative to the Monte Carlo solution for both cases, when the control rod is inserted and withdrawn from the reactor.

Table II. Criticality eigenvalues

Methodology	k-effective (Rod OUT)	Error[a] % (Rod OUT)	k-effective (Rod IN)	Error[a] % (Rod IN)
P_1	0.92663	-5.25	0.93352	-3.0
SP_3	0.95568	-2.28	0.96281	0.04
SP_5	0.95639	-2.21	0.96357	0.12
S_8	0.97705	-0.097	0.96226	-0.01
Monte Carlo	0.9780±0.0006	Reference	0.9624±0.0006	Reference

In Table III we show the calculated control rod worth.

[a] Percentage relative error compared to Monte Carlo.

Table III. Control Rod Worth

Methodology	Control Rod Worth
P_1	-7.96e-3
SP_3	-7.75e-3
SP_5	-7.79e-3
S_8	1.57e-2
Monte Carlo	1.66e-2

The control rod worth calculated with the SP_L methodology is negative, as reported by other authors such as Morel and et al. [8] and P. Kotiluoto. The SP_L calculations yield accurate results for the Control Rod-In case, but when the control rod is replaced with the void region, the k-effective is underestimated by ~2.2% with SP_5. These results contradict the physics of the problem, because a higher k eigenvalue is expected when the control rod is withdrawn. The S_8 transport calculation provides good accuracy compared to Monte Carlo, with an error of -0.01%. These results are consistent with the S_N results presented in the Takeda Benchmark. We observe that the SP_L methodology yields more accurate criticality eigenvalues in the Control Rod-In case, compared to the Control Rod-Out case. Hence, we conclude that the SP_L methodology is more accurate in representing the transport physics of highly absorbing materials as compared to void regions with long streaming mean free paths.

In Fig. 3 we observe a steeper gradient of the flux obtained with P_1, SP_3, and SP_5 in the proximity of the void region, compared to the S_8 solution. This can be attributed to the inability of the SP_L leakage operator to represent the streaming of particles in void regions. For this problem, SP_L overestimates the particle leakage in the void, which consequently leads to the underestimation of k-effective, and therefore yields a negative control rod worth.

In Fig. 3, we show the scalar flux (normalized) at z=8.0 cm and y=2.5 cm in group 1 for the Control Rod-Out case (with the void region in place of the control rod). The flux obtained with the SP_L methodology flattens out in the voided region (caused by the Control Rod-Out) between x=15.0 cm and x=20.0 cm. The maximum error, obtained with P_1 method and compared to the S_8 solution is ~10% at x=15 cm, inside the control rod. In this case, the SP_L equations cannot resolve the angular dependency introduced by the void region when the control rod is withdrawn, even with SP_5 treatment.

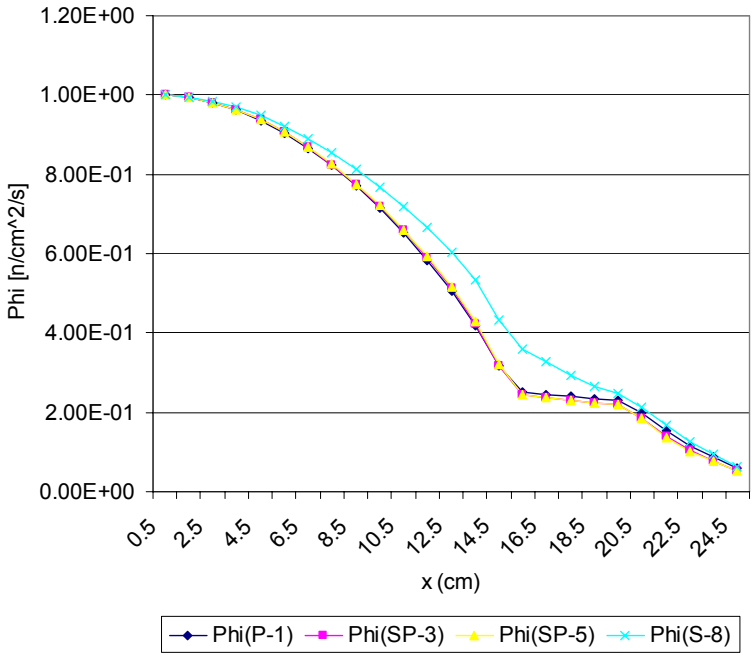

Figure 3. Control Rod OUT - Normalized Flux at z=8.0cm y=2.5cm (Group 1)

In Fig. 4, we show the flux distributions obtained with P_1, SP_3, SP_5 and S_8 at y=2.5 cm and z=8.0 cm, for the case with the Control Rod-In. The SP_L methodology yields accurate flux distributions compared to the S_8 solution. For the Control Rod-In case, the P_1, SP_3 and SP_5 equations yield maximum relative errors equal to 15.3%, 4.5% and 3.4% respectively.

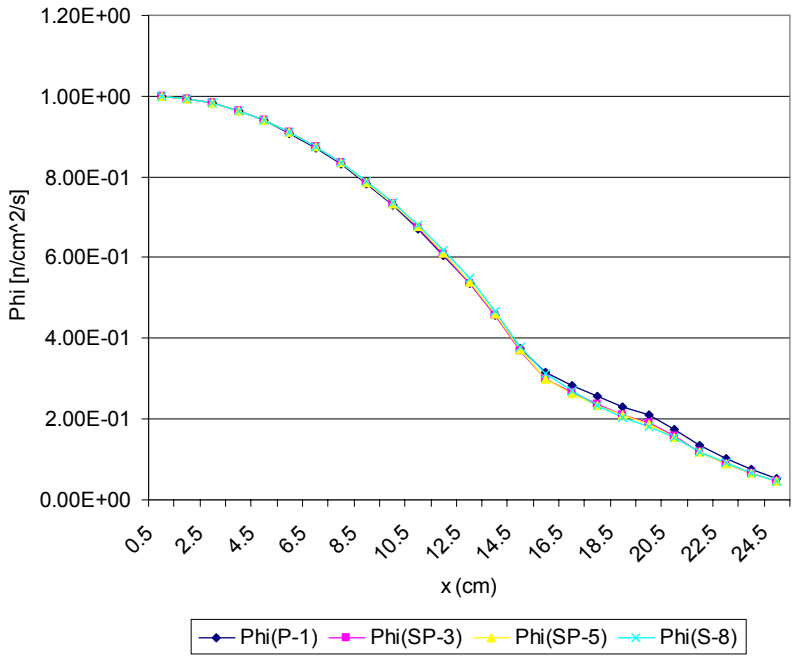

Figure 4. Control Rod IN - Normalized Flux at z=8.0cm y=2.5cm (Group 1)

5. CONCLUSIONS

We have derived the SP_L equations using the even-parity formulation of the transport equation; hence, the SP_L equations have been implemented into the $PENSP_L$ code. The code solves the SP_L equations for fixed source and criticality calculations.

We have compared the accuracy of the SP_L methodology to the discrete ordinates and Monte Carlo methods. The test problem is a criticality benchmark problem originally proposed by Takeda and H. Ikeda; the problem includes two cases: Control Rod-In and Control Rod-Out (causing a voided region), which are challenging situations for the SP_L equations.

We conclude that the SP_L equations are able to represent the physics of highly absorbing media better than for the voided regions. Furthermore, this investigation indicates that for a highly absorbing medium, the P_1 formulation is inaccurate, and at least an SP_3 formulation is needed. While the SP_5 formulation further reduces the noted differences with S_N, the relative gain in accuracy over SP_3 is small compared to the relative increase in the computational cost.

REFERENCES

1. E. Gelbard, J. Davis, and J. Pearson, "Iterative Solutions to the P_l and Double-P_l Equations," *Nuclear Science and Engineering*, **5**, pp.36-44, (1959).
2. G. Longoni, A. Haghighat, and G. Sjoden, "Development and Application of the Multigroup Simplified P_3 (SP_3) Equations in a Distributed Memory Environment," *Proceedings of PHYSOR 2002*, Seoul, Korea, 3-7 October.
3. Sjoden, G. and A. Haghighat, "PENTRAN: A 3-D Cartesian Parallel Sn Code with Angular, Energy, and Spatial Decomposition," *Proceedings of the Joint International Conference on Mathematics and Supercomputing for Nuclear Applications*, Saratoga Springs, New York, **1**, pp.553-562 (1997).
4. E.E. Lewis and G. Palmiotti, "Simplified Spherical Harmonics in the Variational Nodeal Method," *Nuclear Science and Engineering*, **126**, pp.48-58, (1997).
5. P.S. Brantley and E.W. Larsen, "The Simplified P_3 Approximation," *Nuclear Science and Engineering*, **134**, pp.1-21, (2000).
6. J.E. Morel, J.M. McGhee and E.W. Larsen, "A Three-Dimensional Time-Dependent Unstructured Tetrahedral-Mesh SP_N Method," *Nuclear Science and Engineering*, **123**, pp.319-327, (1996).
7. T. Takeda and H. Ikeda, NEACRP-L-330, (1991).
8. E.W. Larsen, J.E. Morel and J.M. McGhee "Asymptotic Derivation of the Multigroup P_1 and Simplified P_N Equations with Anisotropic Scattering ," *Nuclear Science and Engineering*, **123**, pp.328-342, (1996).